Report No.
SAIC-90/1474

Characteristics of Trapped Proton Anisotropy at Space Station Freedom Altitudes

Science Applications International Corporation
An Employee-Owned Company

By

T. W. Armstrong and B. L. Colborn
Science Applications International Corporation

and

J. W. Watts
NASA Marshall Space Flight Center

Work Performed for

NASA Marshall Space Flight Center
Space Science Laboratory, Astrophysics Division
Huntsville, AL.

Contract No. NAS8 - 37916

October 1990

Route 2, Prospect, Tennessee 38477

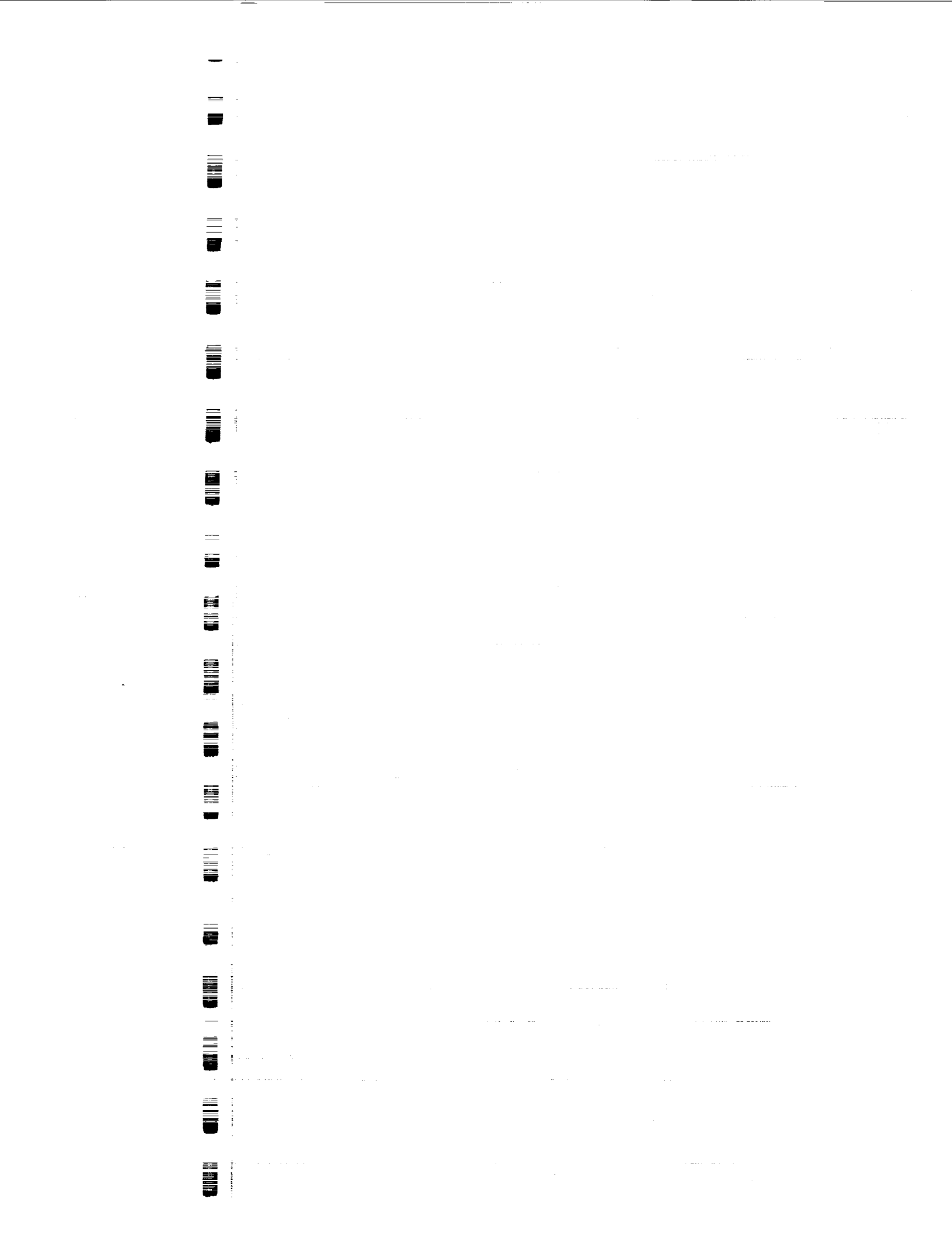

Table of Contents

1. Introduction

The ionizing radiation dose for spacecraft in low-earth orbit (LEO) is produced mainly by protons trapped in the earth's magnetic field (Fig. 1-1). Current data bases describing this trapped radiation environment assume the protons to have an isotropic angular distribution, although the fluxes are actually highly anisotropic in LEO. The general nature of this directionality is understood theoretically and has been observed by several satellites, as summarized in Sec. 2.

The anisotropy of the trapped proton exposure has not been an important practical consideration for most previous LEO missions because the random spacecraft orientation during passage through the radiation belt "averages out" the anisotropy. Thus, in spite of the actual exposure anisotropy, cumulative radiation effects over many orbits can be predicted as if the environment were isotropic when the spacecraft orientation is variable during exposure. However, Space Station Freedom will be gravity gradient stabilized to reduce drag, and, due to this fixed orientation, the cumulative incident proton flux will remain anisotropic (Fig. 1-2). This anisotropy could potentially influence several aspects of Space Station design and operation, such as the appropriate location for radiation sensitive components and experiments, location of workstations and sleeping quarters, and the design and placement of radiation monitors. Also, on-board mass could possibly be utilized to counteract the anisotropy effects and reduce the dose exposure.[1]

Until recently only omnidirectional data bases for the trapped proton environment were available. However, Watts, et al.[2] have developed a method to predict orbit-average, angular dependent ("vector") trapped proton flux spectra from the standard omnidirectional trapped proton data bases.[3] This method has been used here to characterize the trapped proton anisotropy for the Space Station orbit (28.5° inclination, circular) in terms of its dependence on altitude, solar cycle modulation (solar minimum vs. solar maximum), shielding thickness, and radiation effect (silicon rad and rem doses). The method of calculation is described in Sec. 3 and results are given in Sec. 4. While the magnitude of the anisotropy effect at a given internal location is expected to be influenced to some extent by spacecraft geometry, all of the results here are for a one-dimensional (plane) geometry. Calculations to remove this approximation by evaluating anisotropy effects for a three-dimensional model of the Space Station are planned.

An additional output from the calculations here is a data base of vector trapped proton spectra which can be made available as source spectra for use by others to investigate trapped proton anisotropy effects. The contents of this data base is summarized in Sec. 5. A detailed description of the data base and a data retrieval program is given in a companion report.[4]

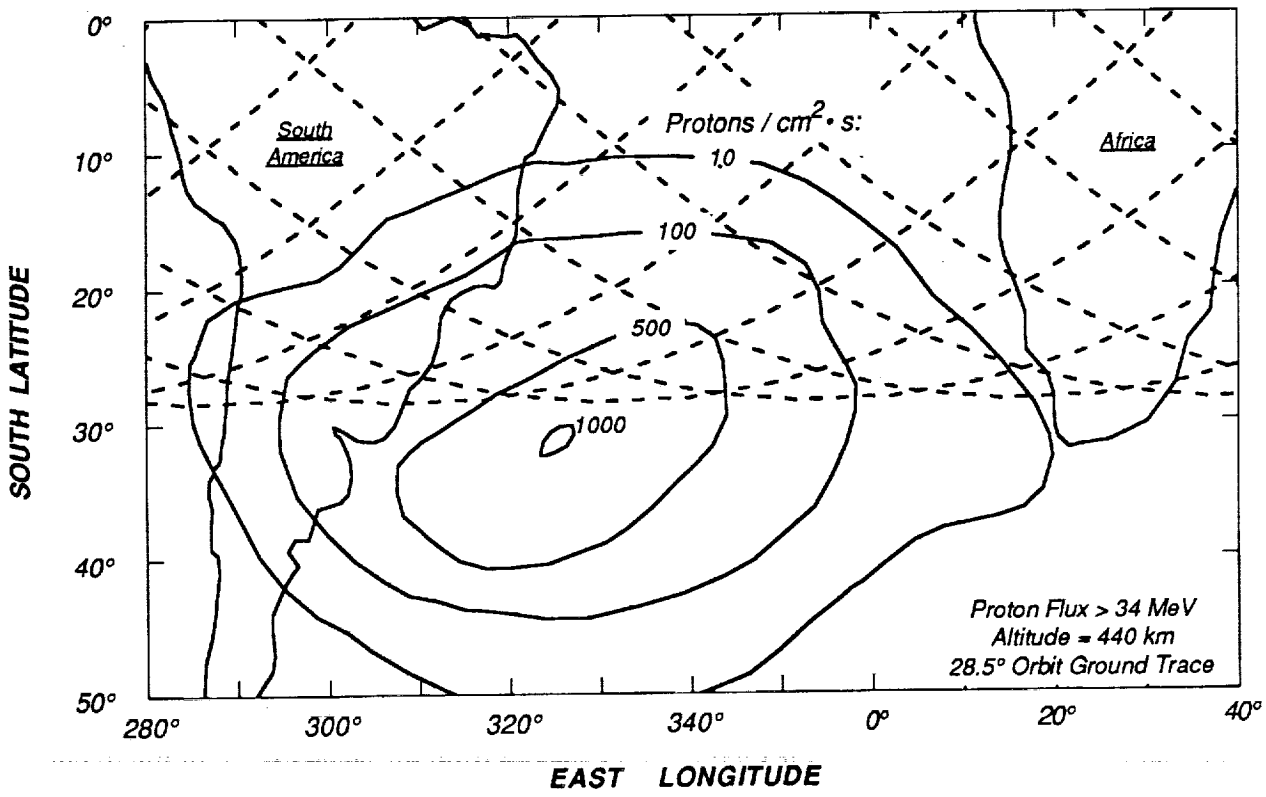

Fig. 1-1. Due to the nonuniform nature of the earth's magnetic field, the trapped proton flux at low altitudes is most intense in the South Atlantic region, as indicated by the iso-flux contours in this figure. Also shown are ground traces (dashed lines) of typical 28.5° inclination circular orbits. Thus, the Space Station, with 28.5° orbits in the 330 to 440 km altitude range, will pass in the vicinity of the most intense region of the trapped proton fluxes, and this will be the dominate source of ionizing radiation dose exposure.

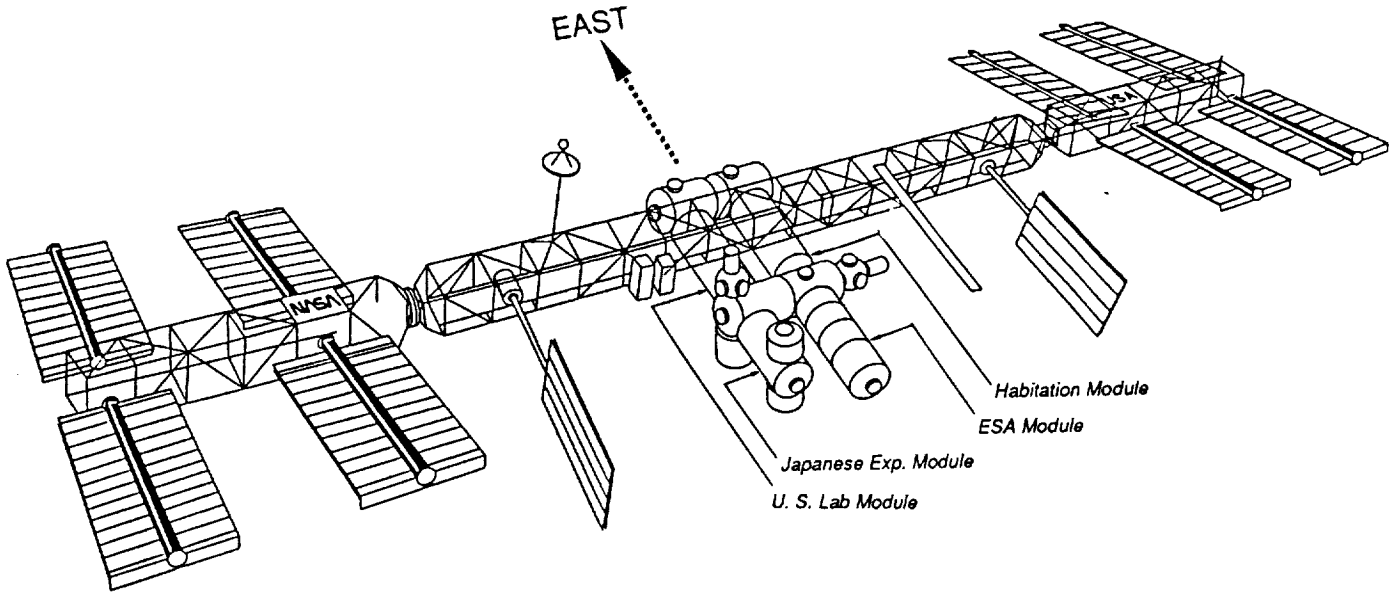

Fig. 1-2. Due to the anisotropy of trapped proton fluxes and Space Station Freedom's fixed orientation in passing through the trapped proton belt, the cumulative radiation intensity incident on the trailing (West) side will be substantially higher than on the leading (East) side. This anisotropy of the radiation exposure may be significant in assessing internal ionizing radiation environments and effects (astronaut dose, potential damage to sensitive materials, background interference to onboard experiments, etc.).

2. Trapped Proton Anisotropy - Background

2.1 Phenomenology

General features of the trapped proton anisotropy are illustrated in Fig. 2-1(a)-(d). For Space Station orbits (28.5° inclination, ~ 300 - 500 km. altitude), the ionizing radiation exposure is dominated by trapped protons in the South Atlantic region, where protons reach lower altitudes due to the nature of the Earth's magnetic field. In this region protons are near their "mirror" points where their trajectories reverse direction and the pitch angle (angle between proton direction and magnetic field line) becomes 90°.

In the mirroring region, proton directions are "planar" since they are confined in planes perpendicular to the magnetic field $\bar{B}$, as illustrated in Fig. 2-1(b). The pitch angle distribution of the proton flux, $j(\theta)$, where the pitch angle θ is measured relative to the normal of $\bar{B}$, can be described as a gaussian with a standard deviation of about 10°.

In addition to the pitch angle distribution, there is a second effect which influences the directionality of trapped protons. In the altitude range of interest the proton radius of gyration is comparable to the atmospheric scale height. Thus, as illustrated in Fig. 2-1(c), protons which gyrate above the point of interest pass through less dense atmosphere, have a lower loss rate from atmospheric interactions, and higher intensity than protons from below. Thus, within a mirror plane there is the "East-West effect" where the proton flux is asymmetric with maximum intensity in the direction of magnetic east (defined by $\bar{B} \times \bar{r}$, where $\bar{r}$ is a vector from the Earth's center to the observation point).

2.2 Theory

Several functional forms have been proposed for the pitch angle distribution describing the planar component of the anisotropy.[5-7] In particular, Heckman and Nakano[7] show that if the density of proton mirror points is assumed to be proportional to atmospheric density, and the atmospheric density is assumed to vary exponentially with altitude, then the pitch angle distribution is gaussian

$$f(\theta)\, d\theta \propto \exp\left[\frac{\theta^2}{2\sigma^2}\right] d\theta$$

with standard deviation

$$\sigma = \sqrt{\frac{3\, h_o\, (2 + \cos^2 I)}{4R}}$$

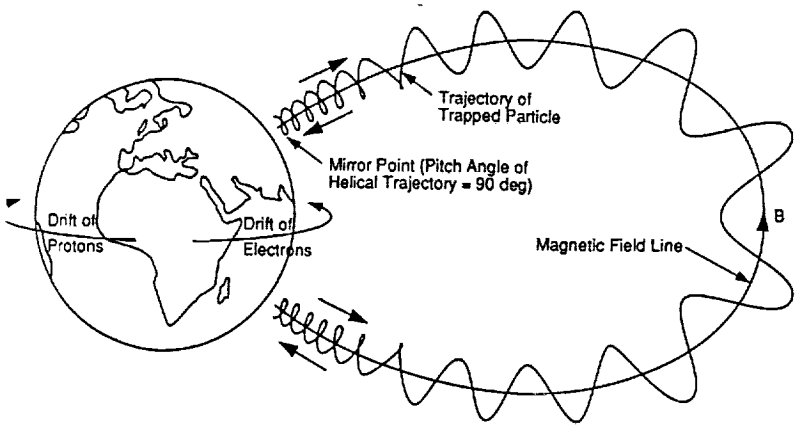

(a) Trapped protons "mirror" in direction when they reach low altitudes and almost all of the Space Station radiation dose will come from orbits passing through this mirroring region.

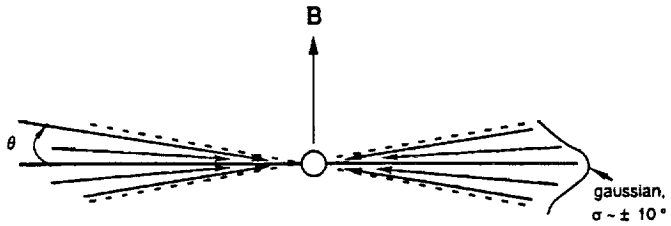

(b) In the mirroring region proton directions are "planar" with pitch angles which can be described by a narrow gaussian distribution perpendicular to the magnetic field line.

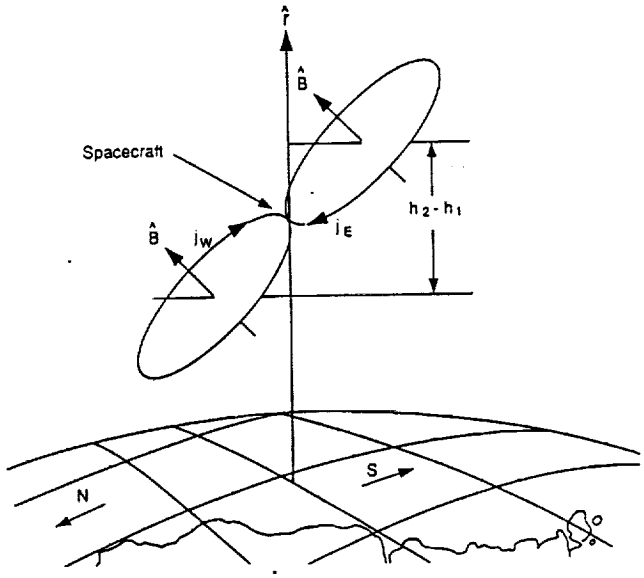

(c) At low altitudes where proton gryradii are comparable to atmospheric density variations, protons gyrating above the observation point about a guiding center at altitude h_2 will pass through lower density atmosphere and have higher intensity than those gyrating below about a guiding center at h_1, so $j_E > j_W$.

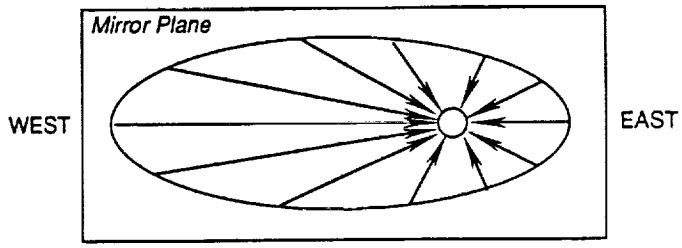

(d) Thus, within the mirror plane the trapped proton flux is asymmetric due to differences in atmospheric losses with the eastward flux higher than the westward flux, which is called the east-west effect.

Fig. 2-1. Basic features of trapped proton anisotropy. Illustrated are the two effects which cause the trapped proton flux at low altitudes to be highly directional: pitch angles near 90° and the east-west asymmetry.

where h_o is the atmospheric density scale height, I is the magnetic field dip angle, and R is the dipolar radius.

The East-West asymmetry was first predicted by Lenchek and Singer.[8] They assumed, as is observed, that the proton flux varies inversely with atmospheric density and that the atmospheric density varies exponentially, which gives

$$\frac{j_2}{j_1} = \exp\left[\frac{h_2 - h_1}{h_o}\right]$$

with h_1 and h_2 the altitudes of the centers of gyration, Fig. 2-1(c), corresponding to protons travelling in directions β_1 and β_2 with respect to magnetic east. The gyrocenter altitudes are determined from

$$h_2 - h_1 = r_g \cos I (\cos\beta_2 - \cos\beta_1)$$

where r_g is the proton gyroradius

$$r_g = \sqrt{E(E + 1876)}/30B$$

with r_g in kilometers, proton energy E in MeV, and the magnetic field intensity B in gauss. The ratio of fluxes in directions β_2 and β_1 within the mirror plane is then

$$\frac{j_2}{j_1} = \exp\left[\frac{r_g \cos I (\cos\beta_2 - \cos\beta_1)}{h_o}\right]$$

which shows that the anisotropy becomes significant when $r_g \geq h_o$. Thus, numerical comparisons of r_g vs. h_o provide an indication of the anisotropy dependence on proton energy (through r_g) and on altitude and solar modulation (through h_o). We infer from such comparisons (Fig. 2-2): (a) the anisotropy increases with increasing proton energy, and will therefore generally increase with increasing shielding depth, (b) for a given proton energy, the anisotropy will be largest at low altitudes where scale heights are smaller, and (c) since the scale height difference between solar minimum and solar maximum is small, the anisotropy dependence on solar cycle will be small. These expected trends are borne out by the detailed calculational results given in Sec. 4.

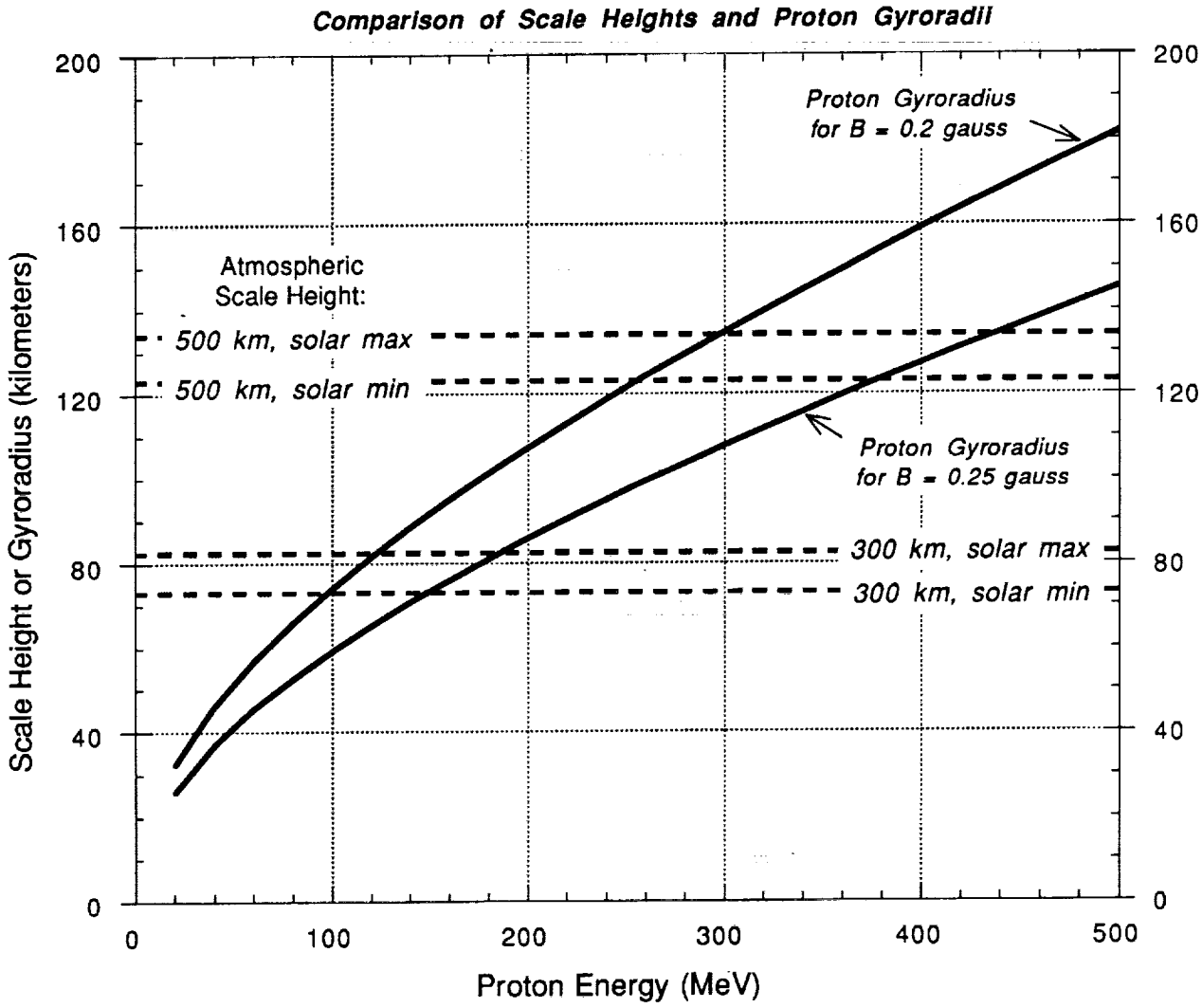

Fig. 2-2. Comparison of atmospheric density scale heights, h_o, at 300 and 500 km altitudes for solar minimum and solar maximum conditions with the energy dependence of proton gyroradii, r_g, for nominal magnetic field intensities at these altitudes in the South Atlantic Anomaly region of the trapped proton belt. The trapped proton anisotropy in terms of the east-west asymmetry becomes important when $r_g \geq h_o$.

2.3 Anisotropy Model

Watts, et al.[2] have used the above relations for proton pitch and mirror plane angular distributions to derive an equation for determining the vector flux spectrum j (E, θ', ϕ). They used a coordinate system fixed to the magnetic field with + z in the direction of $\bar{B}$, + y in the direction of $\bar{B} \times \bar{r}$ (magnetic east), θ' measured from + z, and ϕ measured from + x. Thus,

$$j(E, \theta', \phi) = \alpha\, j_o(E)\, f(\theta')\, j_m(\beta(\theta', \phi))$$

where j_o is the omnidirectional flux, f is the pitch angle distribution, j_m is the angular variation for the east-west asymmetry, $\theta' = \pi/2 - \theta$, and β is related to θ' and ϕ by cos $\beta = \sin\theta' \sin\phi$. The constant α is determined by normalization

$$j_o(E) \equiv \int\int j(E, \theta', \phi)\, d\phi \sin\theta'\, d\theta'.$$

The resulting equation for the vector proton flux spectrum is

$$j(E, \theta', \phi) = j_o(E) \frac{\exp\left[\frac{(\pi/2 - \theta')^2}{2\sigma^2}\right]}{\sin\theta' \sqrt{2\pi}\, \sigma\, \mathrm{erf}\left[\frac{\pi}{2\sqrt{2}\,\sigma}\right]} \frac{\exp\left[\frac{r_g \cos I \cos\beta(\theta', \phi)}{h_o}\right]}{\int_o^{2\pi} \exp\left[\frac{r_g \cos I \cos\beta(\theta', \phi)}{h_o}\right] d\phi}$$

where the integral must be performed numerically.

This equation provides a model for estimating anisotropic trapped proton spectra in the South Atlantic region from currently available environments data bases[3] containing only the omnidirectional spectra j_o (E). The method used by Watts, et al.[2] in implementing this model and the parameter assumptions for present applications are given later in Sec. 3.

2.4 Satellite Observations

There have been various satellite observations of trapped proton anisotropy with different types of instrumentation employed. Pitch angles were measured[9] for $E_p > 350$ MeV by a Cerenkov detector aboard Explorer II, plastic scintillators aboard Gemini 4 measured[10] angular distributions in the energy range $23.5 \leq E_p \leq 80$ MeV, a particle

telescope on the German research satellite Dial measured[5] angular distributions in the energy range $5 \leq E_p \leq 50$ MeV, and measurements using emulsions have been made on numerous Air Force satellites by Fitz and Holeman[11] and by Heckman and Nakano.[12] The measurements by Heckman and Nakano are the most extensive, with emulsions recovered from 27 short duration (2-7 day) polar orbit satellite flights over a four year (1962-1966) period. The altitudes were between about 250 and 500 km during passage through the center of the South Atlantic anomaly. The emulsions measured protons > 57 MeV and the time-dependent satellite orientation was recorded so that both pitch angle and east-west distributions could be extracted. The data were in agreement with the theory of Lenchek and Singer[8] for the east-west asymmetry, and the pitch angle distribution data were well represented by a gaussian with $\sigma = 8°$. A wider pitch angle distribution, $\sigma = 16°$, is obtained from the Fitz and Holeman[11] emulsion data.

These satellite observations clearly show the existence of trapped proton anisotropy and confirm the theoretical concepts. These data are not, however, sufficiently extensive to allow a quantitative test of the accuracy of the anisotropy model given in Sec. 2-3. Such model validation should be possible though from data taken by the recently recovered Long Duration Exposure Facility (LDEF) satellite, as discussed in Sec. 6.

3. Calculational Method

3.1 Atmospheric Scale Heights

Atmospheric density scale heights are needed as an input parameter in applying the Watts, et al. anisotropy model. These scale heights were obtained by using the densities predicted by the MSFC/J70 atmosphere model[13] and then applying a factor derived by Heckman and Nakano[12] for taking into account the average density density over proton trajectory variations at low altitudes due to mirror oscillations and longitudinal drift. The resulting scale height as a function of altitude h in the 250 - 500 km range was fit as $h_o^{min} = 33.4 \exp(h/383)$ for solar minimum and $h_o^{max} = 39.8 \exp(h/412)$ for solar maximum, and these expressions were used to obtain the scale heights used in the calculations here.

3.2 Code System

Except for minor modifications, the code system used for the anisotropy calculations here (Fig. 3-1) is that constructed by Watts, et al.[2]

The omnidirectional trapped proton spectra at solar minimum and solar maximum are taken from the AP8MIN (epoch 1964) and AP8MAX (epoch 1970) data bases.[3] To obtain the magnetic field parameters B and L at points along the orbit needed to extract the omnidirectional fluxes, the ALLMAG magnetic field routines[14] are used. For solar minimum, the International Geomagnetic Reference Field 1965.0, 80-term geomagnetic field model[15], projected to 1964 (the epoch of the omnidirectional trapped proton flux model at solar minimum, was used. For solar maximum, the U.S. Coast and Geodetic Survey 1970, 168-term geomagnetic field model[16] was used.

ORBIT is a version of the MSFC orbit code[17] modified to interface with the magnetic models contained in ALLMAG, to compute the magnetic moment from the field model coefficients in ALLMAG, and to output the omnidirectional fluxes, B-field components, and other orbit parameters at each time step needed for the anisotropy model computations. In the present calculations, one minute time steps and 40 orbits per altitude case were used.

The code VECTOR computes the vector flux spectra at each time step using the anisotropy model equation given in Sec. 2-3. In the present calculations the vector fluxes computed relative to magnetic coordinates were translated to a horizontal geographic

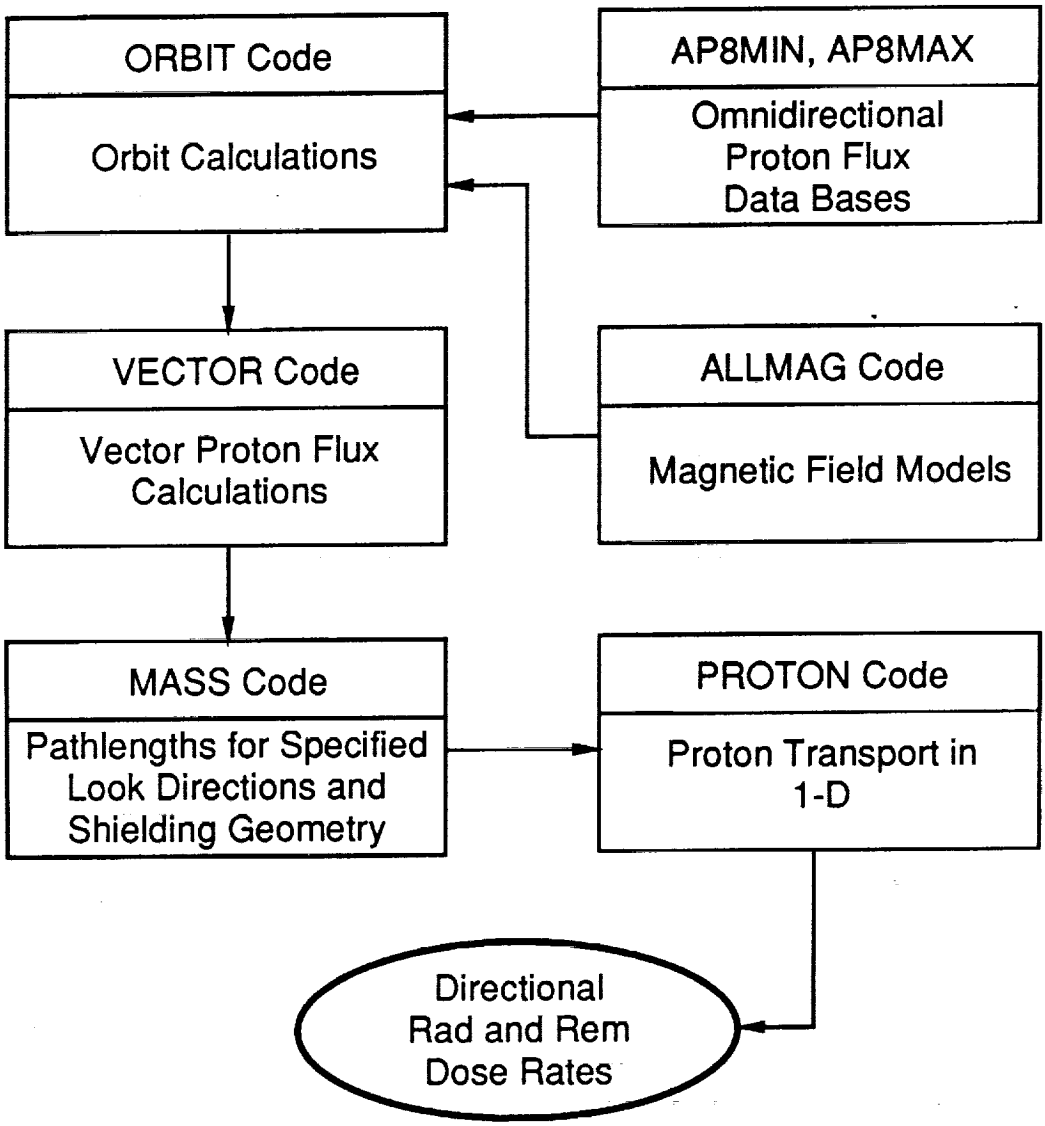

Fig. 3-1. Code system used for trapped proton anisotropy calculations.

coordinate system and then rotated at each time step relative to the spacecraft velocity vector. The output from VECTOR is then orbit-average differential vector flux spectra in a solid angle grid for a spacecraft-fixed coordinate system. The solid angle grid was defined by 20 equal $\cos\theta$ intervals, where θ is measured from the zenith, and 36 φ intervals, where φ is measured from south toward east (Fig. 3-2).

In general, the purpose of the MASS code is to compute the "mass" (areal density) of shielding thicknesses along "rays" projected from a specified observation point through an arbitrary spacecraft geometry in directions corresponding to the vector flux solid angle grid. In the present calculations, a one-dimensional slab shielding geometry is used, and MASS computed the areal density along each of the vector flux directions for a specified shielding depth and "look" direction (corresponding to the orientation of the slab normal).

Dose rates are computed using the Burrell PROTON code,[18] which performs an analytical, one-dimensional proton transport calculation taking into account ionization energy losses with a semi-empirical correction for nuclear collision effects. A separate calculation for the areal density pathlengths along each vector flux direction from MASS is computed and summed with solid angle weighting to obtain the dose at the specified slab thickness. Only directions within a 2π solid angle about the look direction are considered, so the results correspond to a "plane detector" with (effectively) infinite backing. The shielding material here is assumed to be aluminum. Results are obtained for the absorbed dose in silicon and the dose-equivalent (rem) at a depth (5-cm tissue) corresponding to Blood Forming Organs (BFO). Thus, the BFO rem dose at x g/cm^2 shielding depth is computed as the absorbed dose in tissue after x g/cm^2 of aluminum shielding plus 5 cm tissue, times a Quality LET-dependent Factor.[19]

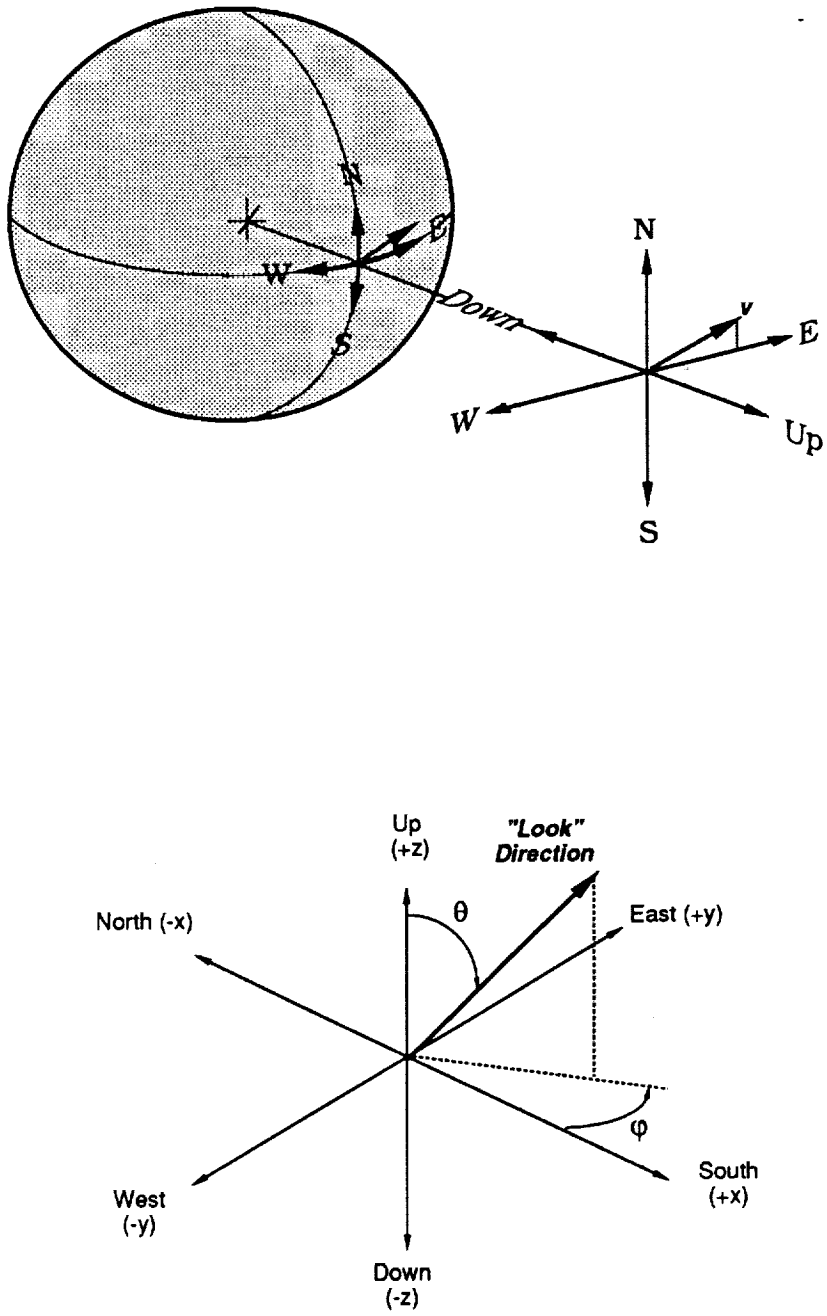

Fig. 3-2. Coordinate system used for trapped proton anisotropy calculations.

4. Results

Given in this section are results from the anisotropy calculations in terms of proton flux, silicon rad dose, and BFO rem dose. All of the results are orbit averages for circular, 28.5° inclination orbits.

4.1. Flux

Fig. 4-1 gives an overview of the integral trapped proton flux over all directions, and Fig. 4-2 shows the angular variation in the horizontal plane (i.e., in the plane perpendicular to the zenith direction) for an example altitude of 450 km. These results show that the vector flux within a differential solid angle has large directional variation. The angular variation in terms of dose will generally be less than for flux because incoming protons over a sizeable solid angle will usually contribute to the dose, so there is some flux-averaging over angle in estimating dose.

Figure 4-3 indicates the altitude dependence of integral fluxes in terms of the ratio of the flux looking west to the flux looking east. For the currently envisioned constant drag strategy, Space Station altitudes are expected to vary from about 330 km. at solar min to about 440 km. at solar max. In this altitude range Fig. 4-3 shows that the west/east ratio of the incident trapped proton flux > 100 MeV, for example, varies from a factor of 10 at 330 km. to a factor of about 6 at 440 km.

4.2 BFO Dose

Fig. 4-4 shows the directionality of the BFO dose for a particular altitude and shielding thickness. As expected, the maximum dose occurs near the horizontal plane (where the proton pitch angles are near 90°) and looking west (where the incident flux is a maximum due to the east-west effect). The minimum dose occurs in two angular regions, corresponding to directions along the magnetic field lines.

Fig. 4-5 shows the west/east anisotropy of the BFO rem dose for different altitudes and shielding thicknesses, and these same results are combined as a contour plot showing the combined shielding and altitude dependences in Fig. 4-6. At the lower Space Station altitude of 330 km., the west side/east side BFO rem dose anisotropy varies from a factor of 3.5 at 1 g/cm^2 shielding to a factor of 6.4 at 20 g/cm^2 shielding. For the higher Space Station altitude of 440 km., the corresponding anisotropy factors are 2.6 and 4.2. These BFO dose ratios, which have been calculated here for radiation incident on one side of a plane geometry, may be lower for actual spacecraft geometries, where radiation incident in directions opposite to the look direction may also contribute.

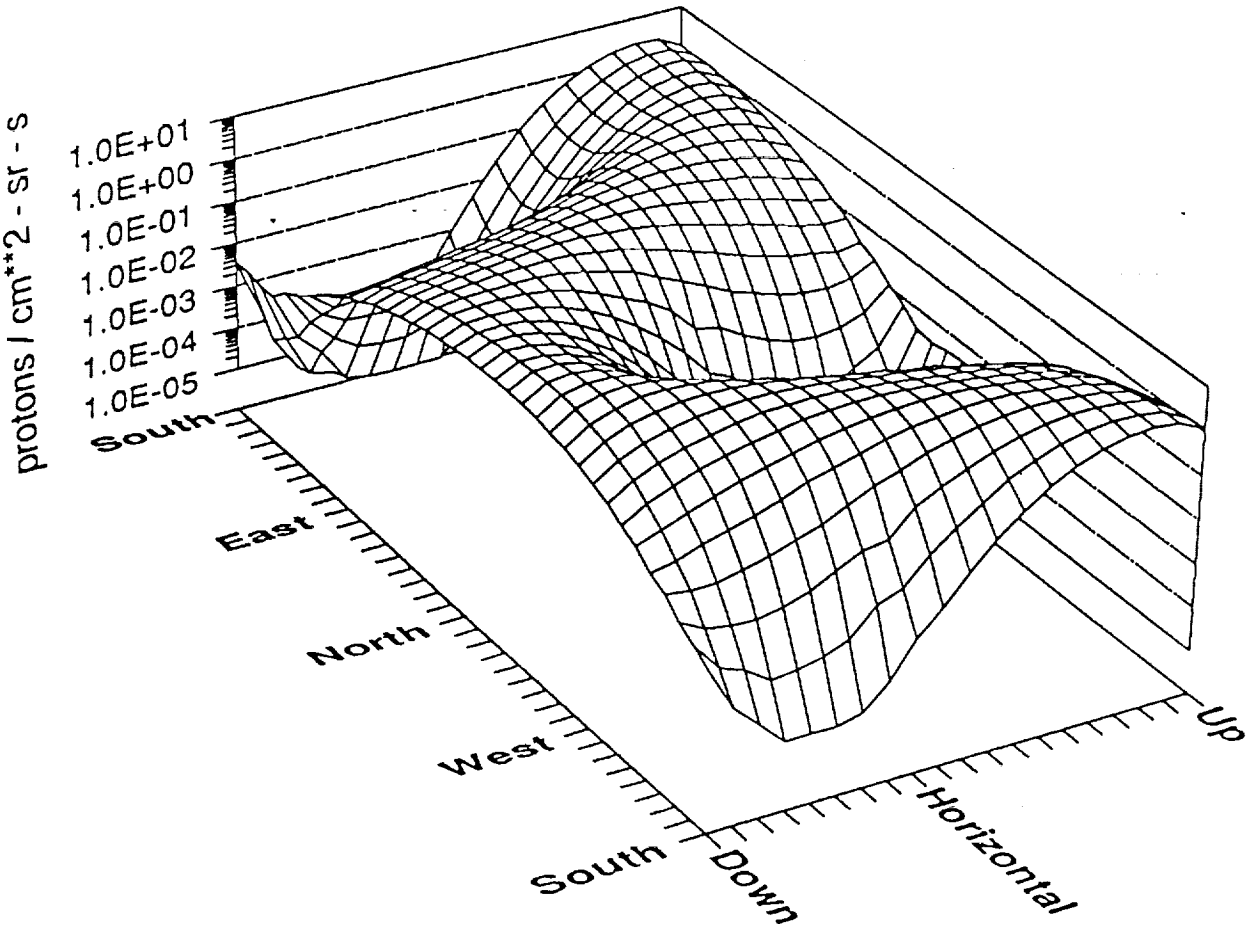

Fig. 4-1. Predicted anisotropy of trapped proton integral flux > 100 MeV (28.5° orbit average, 450 km., solar min).

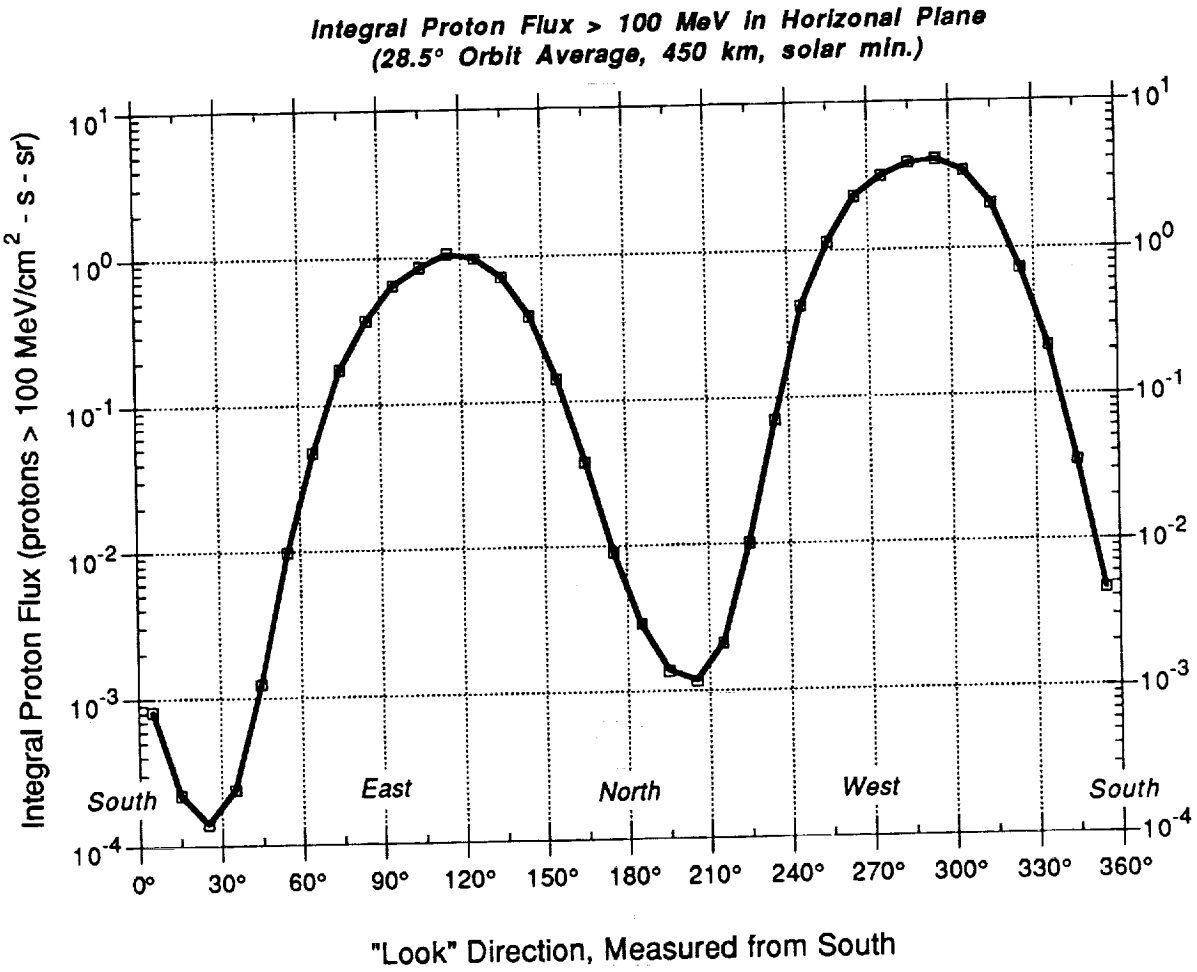

Fig. 4-2. Angular variation of trapped proton ingegral flux > 100 MeV in the horizonal plane perpendicular to the zenith direction (28.5° orbit average, 450 km., solar min).

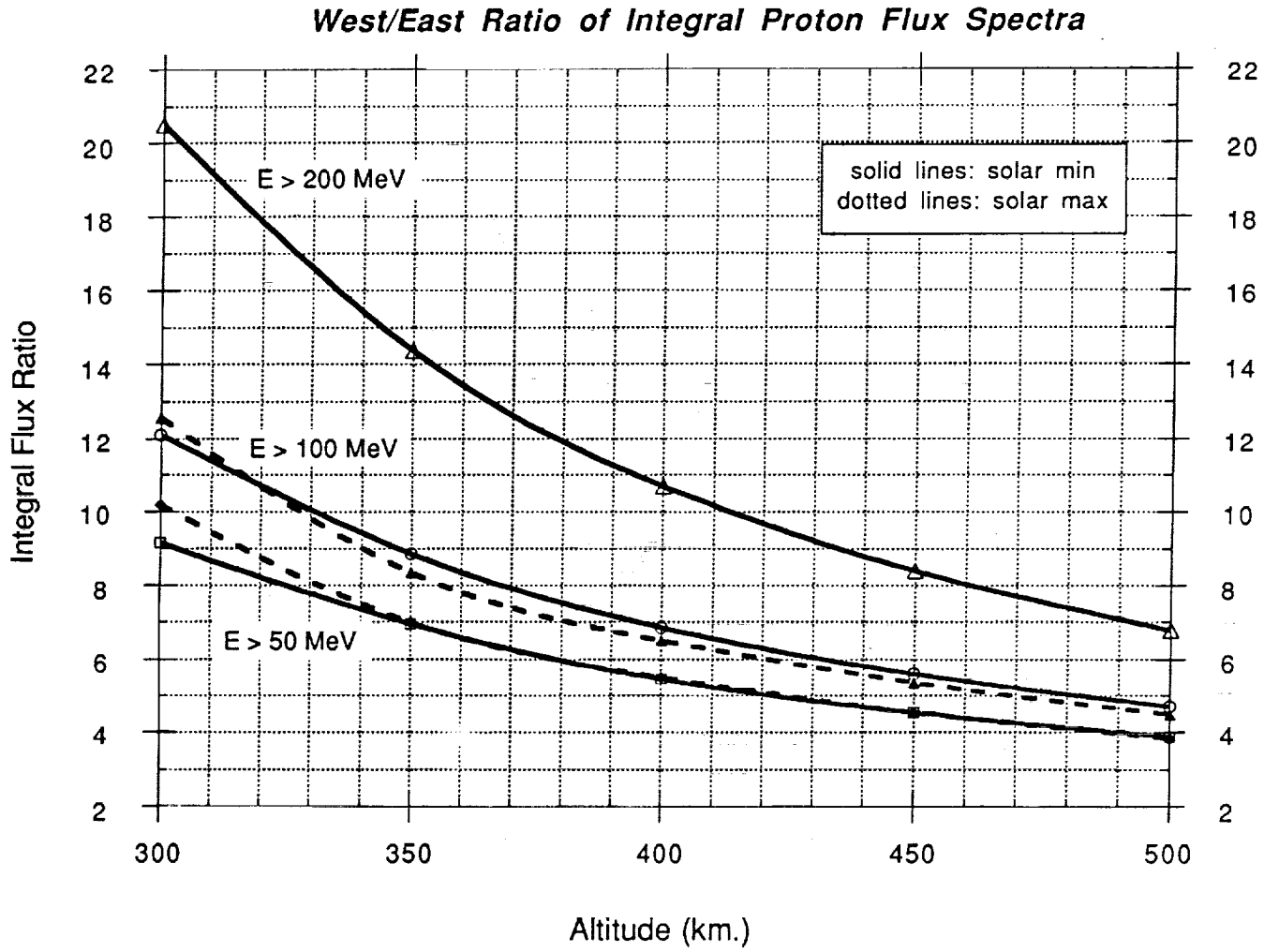

Fig. 4-3. Ratio of the integral trapped proton flux looking west to the flux looking east as a function of altitude.

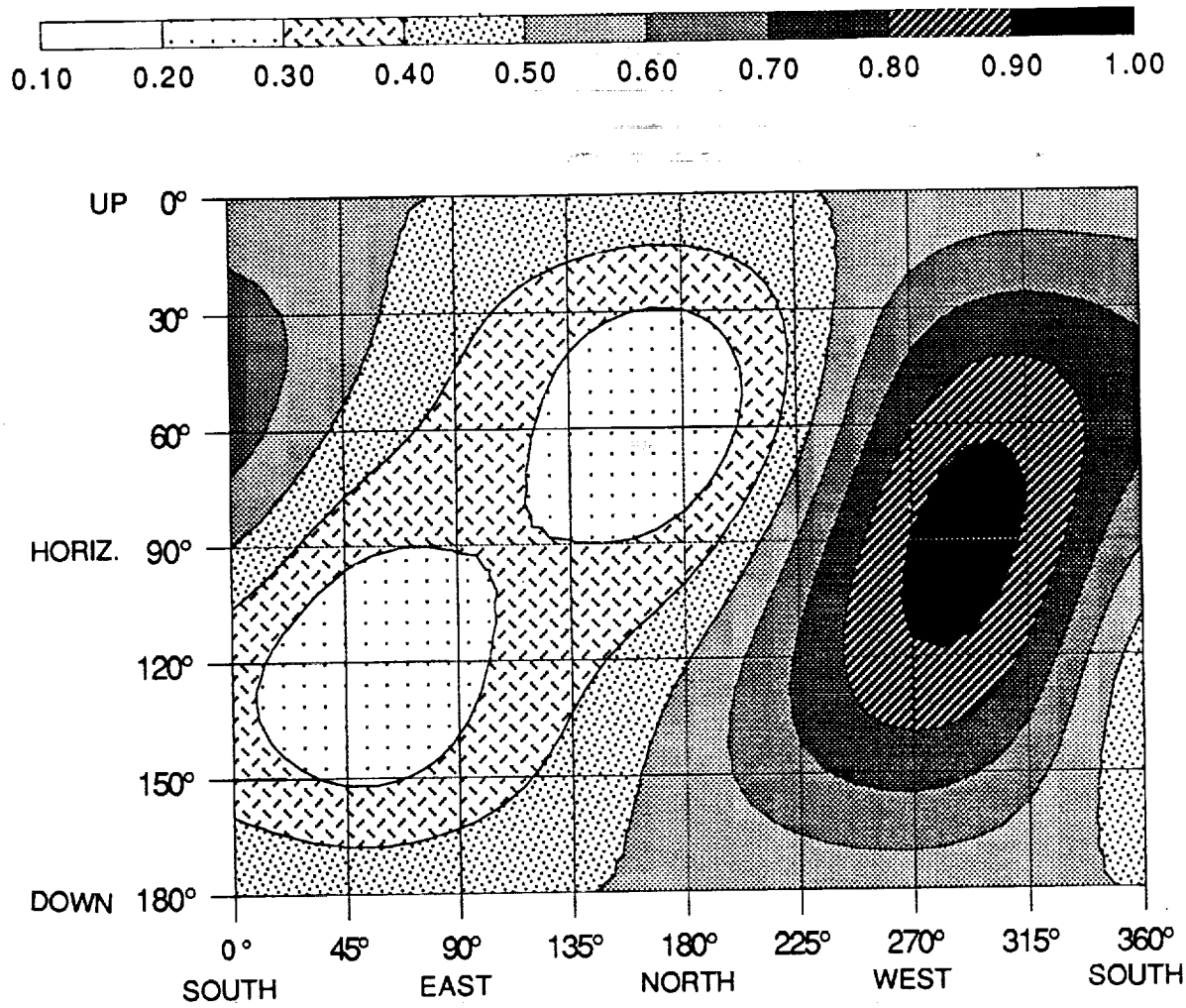

Fig. 4-4. Directionality of the *relative* BFO rem dose behind 5 g/cm^2 aluminum shielding at 400 km. altitude, solar minimum.

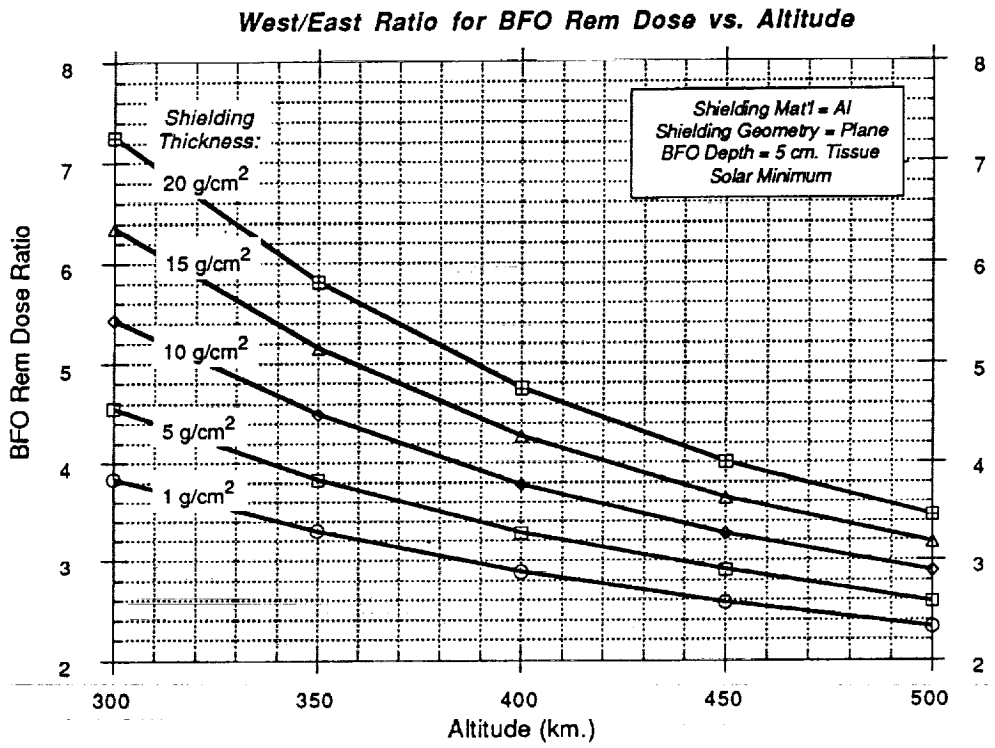

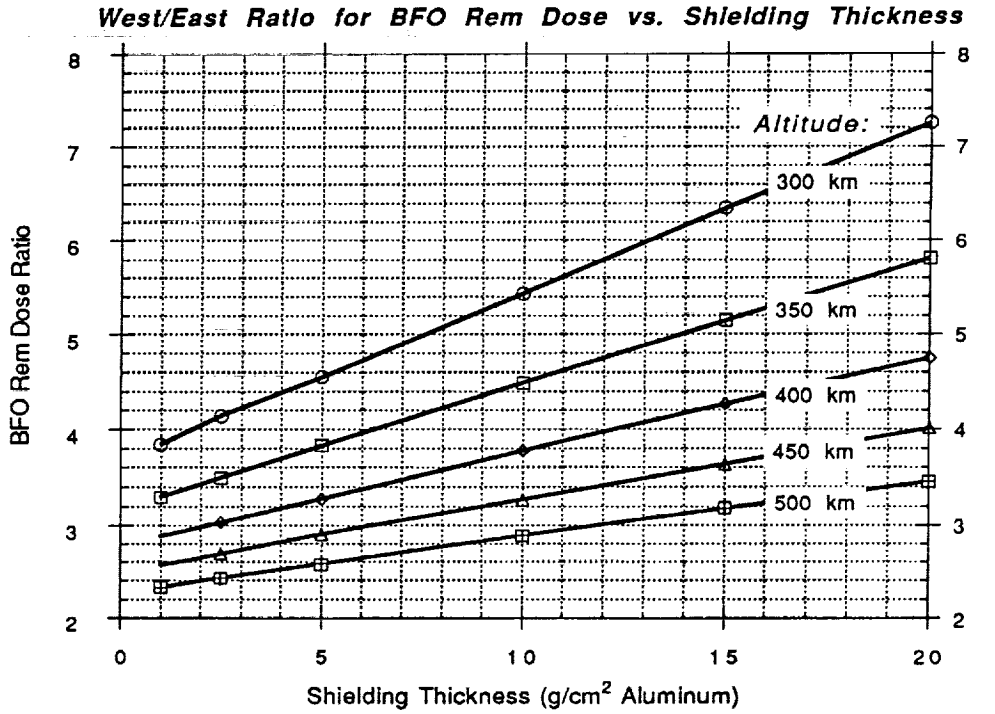

Fig. 4-5. West/east anisotropy of BFO rem dose.

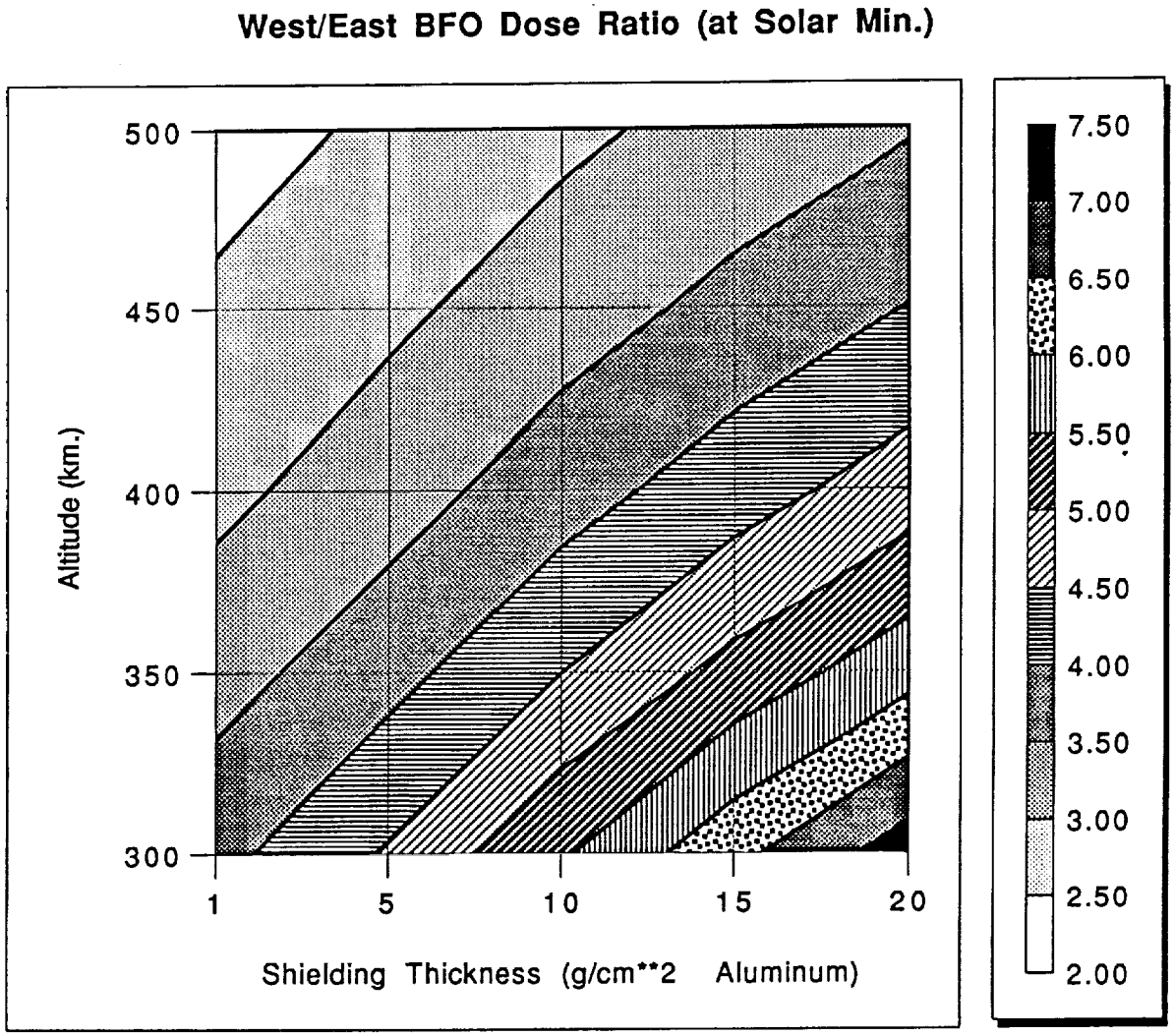

Fig. 4-6. Altitude and shielding dependence of BFO rem dose west/east anisotropy at solar minimum.

4.3 Silicon Dose

Fig. 4-7 shows the east/west anisotropy dependence on altitude and shielding thickness in terms of the absorbed dose in silicon. These curves are similar to those for the BFO dose, but the BFO dose anisotropy is always higher than the silicon dose anisotropy for the same aluminum shielding depth because the calculation of the BFO dose at 5 cm. tissue depth effectively increases the shielding depth for the BFO. Thus, the BFO dose anisotropy will be substantially higher than the silicon dose anisotropy for small shielding depths, but the difference will diminish for large shielding depths, as shown in Fig. 4-8.

4.4 Solar Cycle Dependence

Fig. 4-9 shows that solar modulation does not cause a substantial variation in either the BFO rem or the silicon rad dose anisotropy.

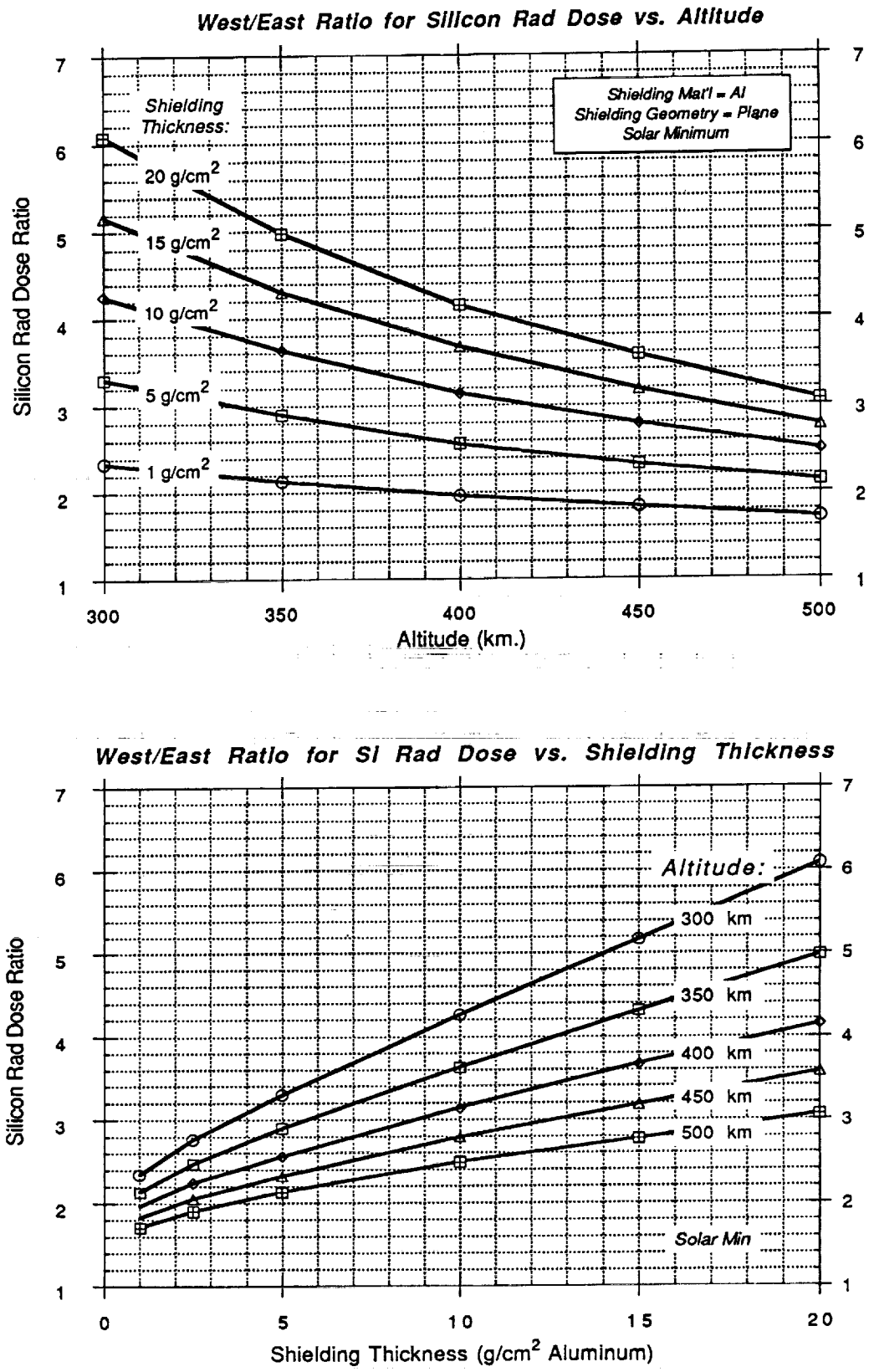

Fig. 4-7. West/east anisotropy of absorbed dose in silicon.

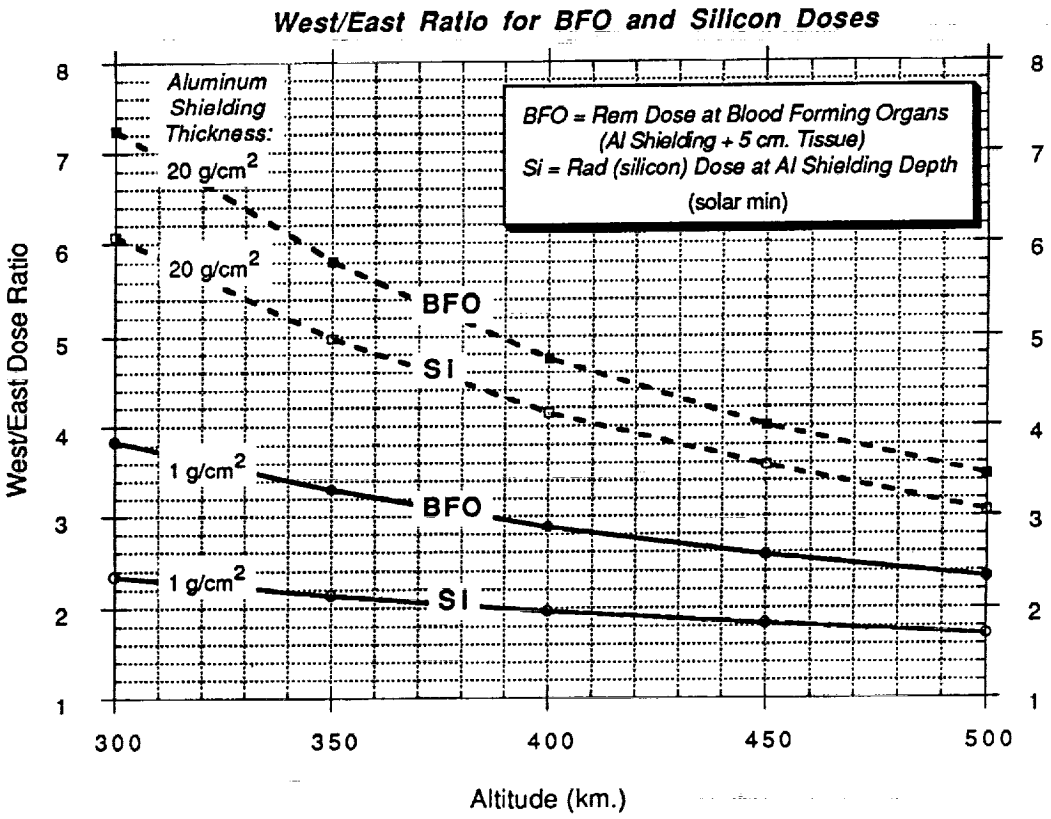

Fig. 4-8. Comparison of west/east anisotropy for BFO rem dose vs. silicon rad dose.

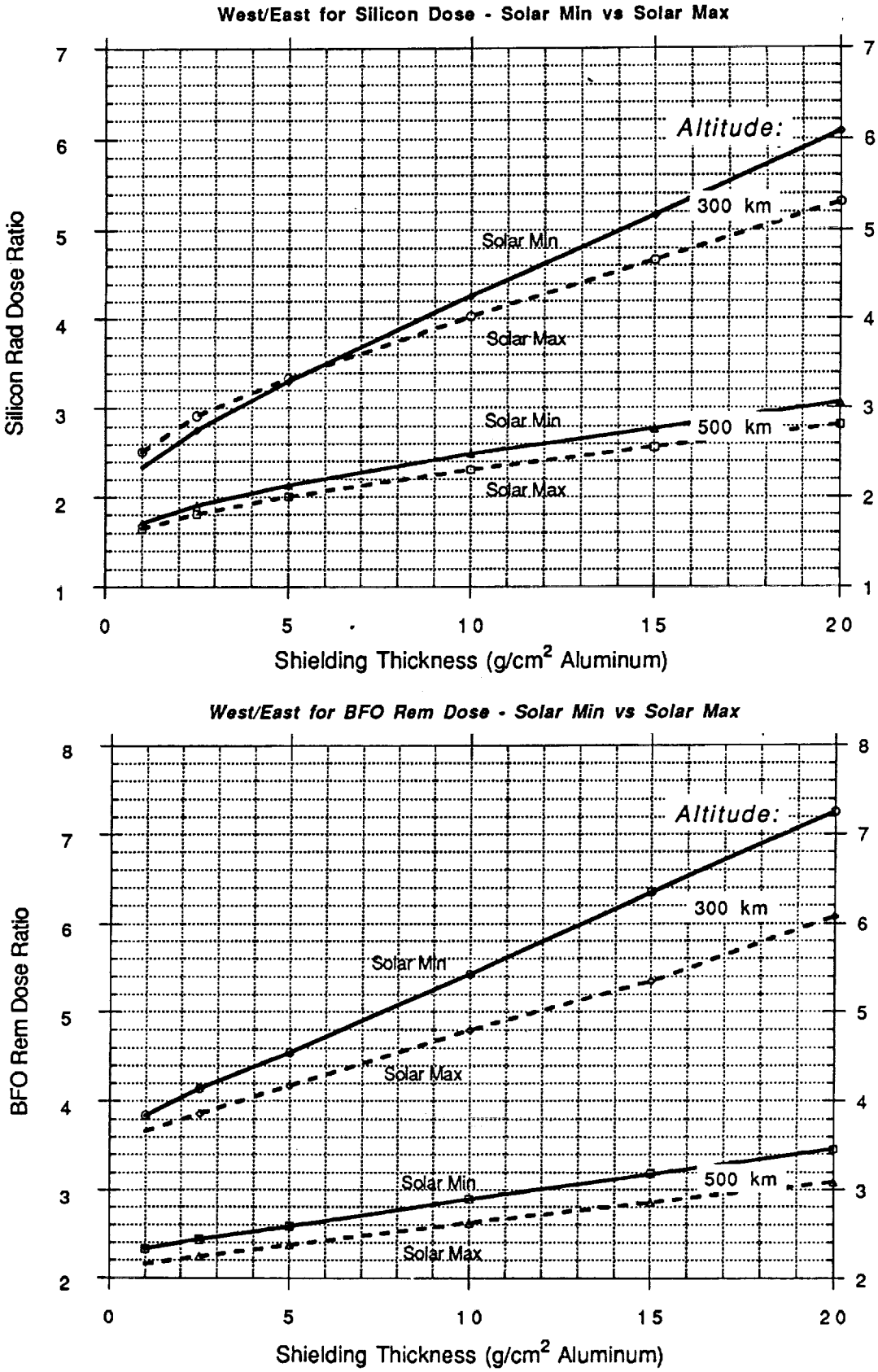

Fig. 4-9. Dependence of west/east anisotropy on solar cycle for silicon rad dose (top) and BFO rem dose (bottom).

5. Vector Flux Data Base

The angular dependent trapped proton spectra for each of the 10 cases calculated here (5 altitudes, solar min and solar max) have been organized into data bases, denoted as VF1MIN and VF1MAX, which can be made available as source spectra for other anisotropy assessments. A summary of the data base contents is given in Fig. 5-1. A detailed description of the data base and a data retrieval program which will allow interface with user transport and radiation effects codes are given in a separate report.[4]

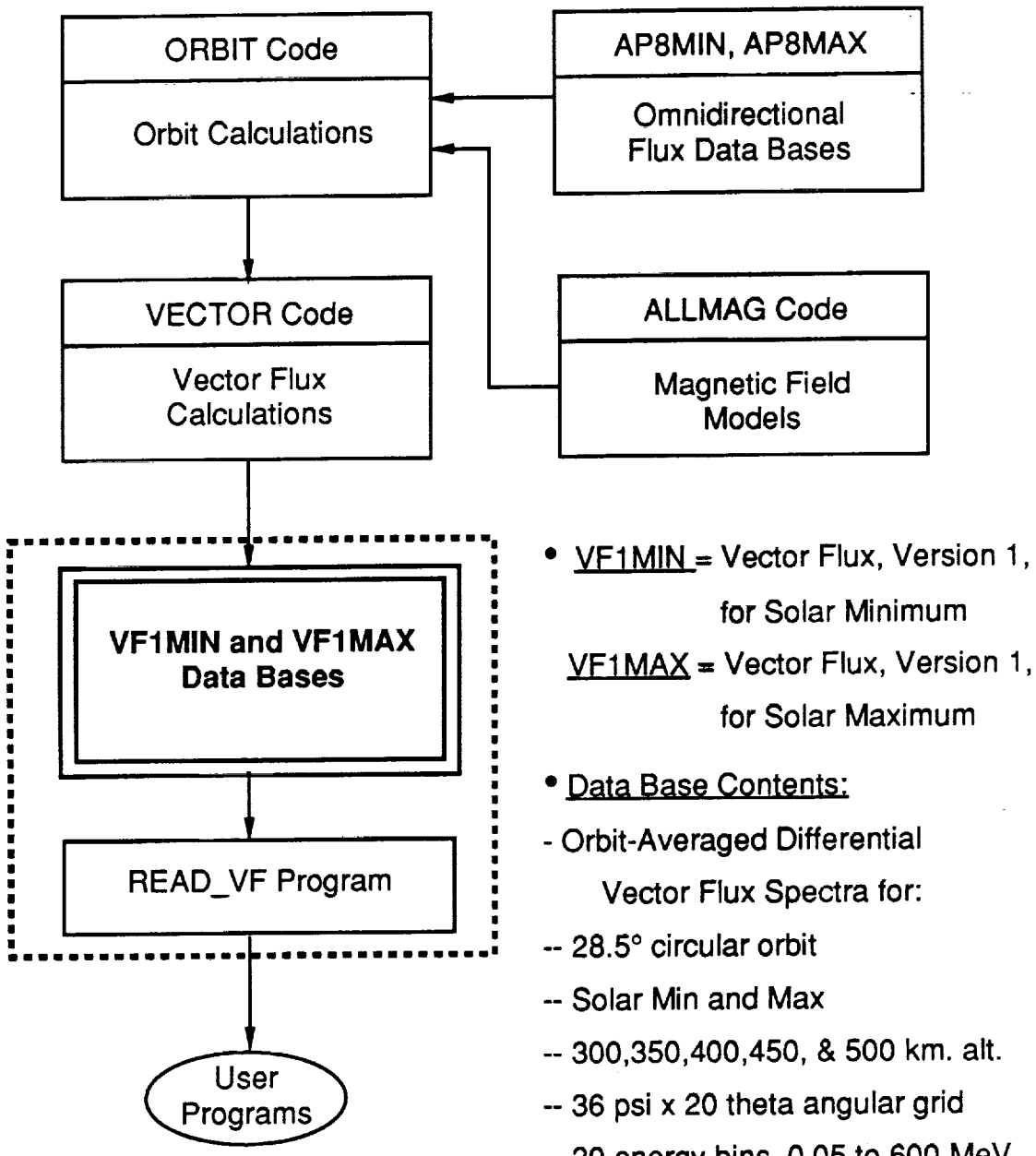

Fig. 5-1. Procedure used in generating the trapped proton vector flux data bases. The data retrieval program READ_VF is provided to allow interface with user transport and radiation effects codes.

6. Discussion

The calculations here show large angular variations in the trapped proton spectra at Space Station altitudes. This results in a substantial dose directionality -- e.g., west/east anisotropy factors of about 3 to 6 for shielding depths ranging from 1 to 20 g/cm^2 in the Space Station altitude range. The dose anisotropy depends strongly on shielding depth and altitude, with only weak dependence on solar cycle.

Two general issues which need to be addressed in further quantifying the trapped proton anisotropy, and in assessing the practical consequences of trapped proton anisotropy for Space Station applications, are higher fidelity simulations and an evaluation of the accuracy of anisotropy model. With regard to simulations, the scoping results here for a one-dimensional shielding model show the anisotropy to be sensitive to shielding thickness, so anisotropy calculations for a realistic three-dimensional Space Station geometry/mass model are needed for a definitive assessment of the anisotropy internal to the Space Station. Also, a more detailed radiation transport treatment taking into account secondary particles is needed to assess the anisotropy of internal radiation environments and its potential influence -- e.g., as background interference to radiation-sensitive instrumentation. To address the simulation fidelity issue, anisotropy calculations using the detailed transport code HETC and a 3-D Space Station geometry model are planned.

With regard to the anisotropy model accuracy, data currently being analyzed from radiation dosimeters aboard the recently recovered Long Duration Exposure Facility (LDEF) satellite provide an opportunity for testing the model. The LDEF data are particularly important for checking the anisotropy model for Space Station applications because the LDEF orbit inclination and altitude range was the same as planned for the Space Station, and the LDEF spacecraft orientation was very stable, with less than 1° wobble over the 5.8 yr. mission duration. Some initial anisotropy calculations for LDEF using the Watts, et al. model have been compared with preliminary LDEF data for the induced radioactivity anisotropy near the spacecraft surface with very good agreement obtained.[20]

7. References

1. Henley, Mark A., "Shielding Distribution for Anisotropic Radiation in Low-Earth Orbit", J. Spacecraft Roc., **23**, 108 (1986).

2. Watts, J. W., T. A. Parnell, and H. H. Heckman, "Approximate Angular Distribution and Spectra for Geomagnetically Trapped Protons in Low-Earth Orbit", Conf. on High-Energy Radiation in Background Space, A. C. Rester, Jr., and J. I. Trombka (Eds.), Santibel Island, FL 1987, AIP Conf. Proc., New York, 1989.

3. Sawyer, Donald M. and James I. Vette, "AP-8 Trapped Proton Environment for Solar Maximum and Solar Minimum", National Science Data Center, Goddard Space Flight Center, NSSDC/WDC-A-R&S 76-06, 1976.

4. Colborn, B. L., T. W. Armstrong, and J. W. Watts, "Data Base Description and Retrieval Program for the Trapped Proton Vector Flux Data Bases VF1MIN and VF1MAX", Science Applications International Corporation Report SAIC-90/1475, October 1990.

5. Fischer, Harald M., Volker W. Auschrat, and Gerd Wibberenz, "Angular Distribution and Energy Spectra Protons of Energy $5 \leq E \geq 50$ MeV at the Lower Edge of the Radiation Belt in Equatorial latitudes", J. Geophys. Res., **82**, 537-547 (1977).

6. Badhwar, Gautam D. and Andrei Konradi, "Conversion of Omnidirectional Proton Fluxes into a Pitch Angle Distribution", J. Spacecraft and Roc. **27**, 350 (1989).

7. Heckman, Harry H., and George H. Nakano, "East-West Asymmetry in the Flux of Mirroring Geomagnetically Trapped Protons", J. Geophys. Res., **68**, 2117-2120 (1963).

8. Lenchek, A. M., and S. F. Singer, "Effects of the Finite Gyroradii of Geomagnetically Trapped Protons", J. Geophys. Res., **67**, 4073 (1962).

9. Garmire, Gordon, "Geomagnetically Trapped Protons with Energies Greater Than 350 MeV", J. Geophys. Res., **68**, 2627-2638 (1963).

10. Reagan, J. B., and W. L. Imhof, "Observations of the East-West Asymmetry Protons Trapped at Low Altitudes", XIII Plenary Meeting of Cospar, Czechoslovakia, (1969).

11. Fitz, Robert and Ernest Holeman, "Time and Altitude Dependence of 55-MeV Trapped Protons, August 1961 to June 1964", J. Geophys. Res., **70**, 5804-5821 (1965).

12. Heckman, H. H. and G. H. Nakano, "Direct Observations of Mirroring Protons in the South Atlantic Anomaly", Space Research V, Proceedings of the Fifth International Space Science Symposium, 329-342 (1964).

7. References (cont'd)

13. Johnson, Dale L. and Robert E. Smith, "The MSFC/J70 Orbital Atmosphere Model and the Data Bases for the MSFC Solar Activity Prediction Technique", NASA TM-86522, November 1985.

14. Stassinopoulos, E. G. and Gilbert D. Mead, "ALLMAG, GDALMG, LINTRA: Computer Programs for Geomagnetic Field and Field-Line Calculations", National Space Science Data Center, Goddard Space Flight Center, NSSDC 72-12, February 1972.

15. IAGA Commission 2 Working Group 4 Analysis of the Geomagnetic Field, International Geomagnetic Reference Field 1965.0, J. Geophys. Res., **74**, 4407 (1969).

16. Hurwitz, Louis, Mathematical Model of the 1970 Geomagnetic Field, ESSA Coast and Geodetic Survey, May 1970.

17. Burrell, M. O. and J. J. Wright, "Orbital Calculations and Trapped Radiation Mapping", NASA TM X-53406, March 1966.

18. Burrell, Martin O., "The Calculation of Proton Penetration and Dose Rates", NASA TM X-53063, August 1964.

19. International Council on Radiation Protection, Publ. 26, Pergamon Press, Oxford (1977).

20. Armstrong, T. W. and B. L. Colborn, "Scoping Estimates of the LDEF Satellite Induced Radioactivity", Science Applications International Corporation Report SAIC-90/1462, September 1990.